Journal of ELECTRICAL ENGINEERING, VOL 73(2022), NO6, 405–412

sciendo

PAPERS

Performance of closed-form equations for force between cylindrical magnets over wide range of volume, aspect ratio, and force

Stan Zurek[1]

Four types of magnets were used in this study: neodymium NdFeB (grade N35 and N52), ferrite (Y10), and samarium-cobalt SmCo (XG30 2:17). They were chosen to represent a wide range of volumes from 0.035 to 19 cm^3 (540 times), radius R from 1.5 to 12.5 mm (8 ×), length L from 0.5 to 40 mm (80 ×), aspect ratio L/R from 0.051 to 17 (330 ×), and contact forces from 0.2 to 250 N (over 1000 ×). The study shows that previously reported closed-form equations are valid only at large distances (small forces). At short distances (large forces) the calculated force diverges to infinity or the accuracy depends on the aspect ratio, and some equations fail more than others. A new equation is proposed as a small modification of a previously known function, which provides reasonable behaviour over the whole studied range. However, the accuracy is unknown in a general practical case, because theoretical calculations do not take into account imperfections of real magnets, so there is no single absolute reference.

K e y w o r d s: closed-form equations, cylindrical magnets, forces between magnets, magnetic forces

1 Introductioon

Magnetic interactions between permanent magnets can be calculated from Maxwell's equations, which can be solved analytically only for the simplest of geometries. Cylindrical magnets can be treated analytically by quite complex integrals [1-6], and provide good agreement with experiments and with numerical finite-element methods (FEM) [7]. However, the analytical and numerical techniques require dedicated mathematical software, which is not necessarily straightforward in practical use [7]. Therefore,closed-form equations are sought-for entities, because they can be easily deployed with commonly used engineering tools such as spreadsheet calculators.

2 Closed-form equations

Several authors proposed closed-form equations for calculating the axial force acting between two identical axially magnetized cylindrical magnets, placed on a common axis, Fig. 1. The resulting force can be either repelling or attracting, depending on the polarity.

2.1 Equations for curve $F = f(x)$

One approach is to treat the magnets as point-like magnetic dipole moments m , which are related to the magnetization M and volume of the cylindrical magnet V, as in (1). However, the value of M is typically not available but can be calculated from the remanent flux density B_r [8, 9], which is typically given for commercially available magnets, and so it can be used directly. Thus, with μ_0 being permeability of vacuum it can be written $M = B_r/\mu_0$.

$$m = MV = \frac{B_r}{\mu_0}\pi R^2 L\,, \tag{1}$$

where, M – magnetization, $V = \pi R^2 L$ – volume of the cylindrical magnet, R – cylinder radius, L – cylinder length.

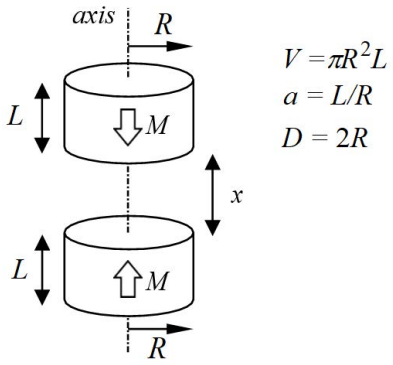

Fig. 1. Two co-axial cylindrical magnets (repelling): $a = L/R$ – aspect ratio, D – magnet diameter, L – magnet length, M – magnetization, R – magnet radius, V – magnet volume, x – separation (gap) between magnets

If the separation x between magnets is much greater than their size ($x >> L$, but also $x >> R$) then the size of dipoles can be ignored (ie treated as "points") and the force can be approximated [9-13],

$$F_{\text{Cast}} = \frac{3\mu_0 m^2}{2\pi x^4} = \frac{3\pi B_r^2 L^2 R^4}{2\mu_0 x^4}\,. \tag{2}$$

[1] Encyclopedia Magnetica, Po Box 1042, City Road, EC1V 2NX, London, United Kingdom, stan.zurek@ieee.org

https://doi.org/10.2478/jee-2022-0055, Print (till 2015) ISSN 1335-3632, On-line ISSN 1339-309X

which is also given here converted to input values available commercially, as mentioned above.

It should be noted that (2) cannot be used for calculation of contact force (ie magnets touching each other, $x = 0$) because it diverges to infinity. However, in a general case it is unknown in practice over which range the equation is valid, and where it diverges too much to be useful. For clarity, results of (2) will be referred to as *Castaner*, after [9].

In [11] (*Furlani*), used an approach based on "magnetic charges" concentrated on the circular surfaces, with the positive terms denoting the repulsion and the negative terms the attraction, and the total force is the net sum of the contributing factors

$$F_{\mathrm{Fur}} = \frac{\pi B_r^2 R^4}{4\mu_0}\Big(\frac{1}{x^2} + \frac{1}{(2L+x)^2} - \frac{2}{(L+x)^2}\Big). \qquad (3)$$

The following equation, from [13] (*Cheedket*) behaves more correctly, providing a value for $x = 0$ (ie contact force F_0). However in [11], the value of B_r was fitted to the experimental data, so the predictive capability of this equation was not proved, despite seemingly good agreement of the curve shape with experiment over the investigated range. However, as shown below, the shape of this curve is ill-behaved for low aspect ratio (ie coin-like magnets) and small distance

$$F_{\mathrm{Chee}} = \frac{\pi B_r^2 R^2}{2\mu_0}\Big(\frac{2(L+x)}{\sqrt{(L+x)^2+R^2}} - \frac{2L+x}{\sqrt{(2L+x)^2+R^2}} - \frac{x}{\sqrt{x^2+R^2}}\Big). \qquad (4)$$

Another equation from [7] (*Schomburg*) is applied to cuboidal magnets, but is included here because of its simplicity. Unfortunately, values F_0 (contact force) and d_e (distance at which $F(d_e) = F_0/4$) are unknown, and real forces have to be measured and curve-fitted before calculations can be carried out, or these values have to be provided from other equations, which limits the applicability of this approach

$$F_{\mathrm{Sch}}(x) = F_0 \frac{d_e^2}{(x+d_e)^2}\,. \qquad (5)$$

For large distances, the force should be proportional to $1/x^4$ slope regardless of the shape of the magnets, yet no such proportionality can be expected from (5). Hence, it works reasonably only for relatively small distances, but it is not possible to know where the equation begins to fail in practice.

In this paper the author also proposes a modified function (*new*)

$$F_{\mathrm{new}}(x) = \frac{\pi B_r^2 R^4}{4\mu_0}\Big(\frac{1}{x_C^2} + \frac{1}{(2L+x_C)^2} - \frac{2}{(L+x_C)^2}\Big)\,. \qquad (6)$$

which is based on (3). The general mathematical expression is the same, but with the input variable x modified to $x_c = x + c$, by the length scaled by the aspect ratio such that $c = bL/a$ where b is a constant fitting coefficient. The c is a constant for a given geometry of magnets, reducing to $c = Rb$, and can be set as $c = 4R/5$, thus $x_c = x + 4R/5$. The value of 4/5 has no "physical" meaning other than obtaining reasonable balance between curve fit and contact force F_0.

This equation was not derived in any strict way, but simply applied in order to reduce the divergence to infinity for $x = 0$. Yet, as shown below, it offers reasonable behaviour over the whole range of distances, aspect ratios, and forces, including predictive capabilities, and calculation of the contact force F_0 .

2.2 Equations for contact force $F_0 = f(0)$

There are also equations, which aim only at predicting the contact force F_0, without representing the whole curve. The following equation was originally derived in [1] (*Agashe*), but it contained a printing error, which was probably found out by Vokoun *et al* [14] so that a corrigendum was issued [15]. A simplified version is further converted here

$$F_{\mathrm{Aga}} = \frac{\pi B_r^2 R^2 L}{64\mu_0\sqrt{R^2+L^2}}\Big(32 + \frac{3R^4}{(R^2+L^2)^2} - \frac{9R^8+12R^6L^2}{(R^2+L^2)^4}\Big). \qquad (7)$$

In [14], (*Vokoun*) are employed complete elliptic integrals, which are not closed-form as such, but they can be approximated with closed-form functions, with some reasonable accuracy

$$F_{\mathrm{Vok}} = \frac{2\pi B_r^2 RL}{\mu_0}\Big(\frac{E(l_1)-K(l_1)}{l_1} - \frac{E(l_2)-K(l_2)}{l_2}\Big) \qquad (8a)$$

where, $K(\dots)$ and $E(\dots)$ – complete elliptic integrals of the first and second kind, respectively, also $l_1 = \big(1 + (L/R)^2\big)^{-1/2}$ and $l_2 = \big(1 + (L/2R)^2\big)^{-1/2}$.

An example of closed-form approximations for the complete elliptic integrals, with 0.5% error is given for instance in [16],

$$K(l) = \frac{\pi}{2(1-l)^{0.19}} - 0.17(l+0.015)^{0.8} \qquad (8b)$$

$$E(l) = \frac{\pi}{2} - 0.567\, l^{2.4+(l+0.1)^{5.8}} \qquad (8c)$$

These approximating functions are used hereinbelow on purpose (rather than the accurately calculated elliptic integrals) in order to indicate the kind of error which can be expected from such closed-form simplification.

The author would like to stress here, that the discrepancies of the values referred to in this paper as *Vokoun* result mostly from the imperfect approximations of elliptical integrals 8(b),(c) and not due to any incorrectness of 8(a) as such. As shown below, these errors can be surprisingly large (despite the 0.5% accuracy of approximation of the integrals themselves). When proper integrals are used then the results of *Vokoun* 8(a) are very close to *Agashe* (7), but these are not repeated here, for brevity.

2.3 Online tools

The online tools typically do not disclose any equations, but they can be easily accessed and conveniently used, so the results of some of them are included here just as additional references. There are several online tools provided by magnet manufacturers and/or distributors. A popular tool [17] is based probably on a numerical integration (as can be judged from the code included in the webpage), but large differences for identical magnets and *almost* identical magnets makes the validity of this particular approach questionable and thus not used in this study.

An example of a more trustworthy tool is [18] ($K\&J,$) which computes repelling (or attracting) force over a range of separation, including the contact force F_0. The exact method of calculation is not disclosed, but it is stated on their website that: "This page calculates expected pull forces based on extensive product testing", and $K\&J$ confirmed to the author that they use proprietary equations based on extensive measurements as well as FEM [19]. $K\&J$ tool provides both repelling and attracting forces (which differ slightly, as they should due to magnet permeability being slightly greater than unity), and is sometimes used as a "reference" also by other researchers, *eg* for Ansys [20]. It also is used here for the same purpose, especially that it provides repulsive force for smaller distances.

Another example is [21] (*Supermagnete*), for which the calculation method is disclosed as based on FEM and only provides values for attracting force at various distances. Assuming that the repulsive and attractive forces are equal in the first approximation, the results can be compared to other sources. There are also several calculators which give "pull force" or contact force F_0, only at $x = 0$. Those used in this paper are [22] (*Dura*) and [23] (SDM), and they also do not disclose the equations, but they can be used simply for comparison.

2.4 Finite-element method FEM

As an additional reference, 2D FEM simulations were employed in axisymmetric mode, which correctly represents the 3D case due to rotational symmetry. Unfortunately, FEMM [24] requires that a given part is surrounded by air before the force acting on it can be calculated, which prohibits the calculation of contact force. An arbitrary decision was made to use a separation of 0.1 mm as a proxy for the "contact force". Investigation of analytical curves, $K\&J$, and *Supermagnete* shows that the difference in force between 0.1 mm and 0 mm is less than 10%, which is mostly small when compared with other differences, as evident from the figures.

3 Experimental

3.1 Note on the experimental approach

It should be clarified here that the measurements carried out in this study were not meant to be used as the direct experimental validation for the analytical calculations. The reason is that the actual parameters of the real magnets can never be known with perfect accuracy. At best, the nominal B_r value is provided, which for N35 magnets can differ by 6.8% [25] which would impact the forces by 14%. Additionally, the dimensions of magnets are not precisely cylindrical. All the magnets have visibly imprecise corners (see especially Fig. 2(c) and Fig. 2(e). The NdFeB magnets are covered with a layer of ferromagnetic coating (0.03 mm thick as measured by the author), which contributes by some unknown amount to lowering the total magnetic field outside of the magnet and therefore also the acting forces.

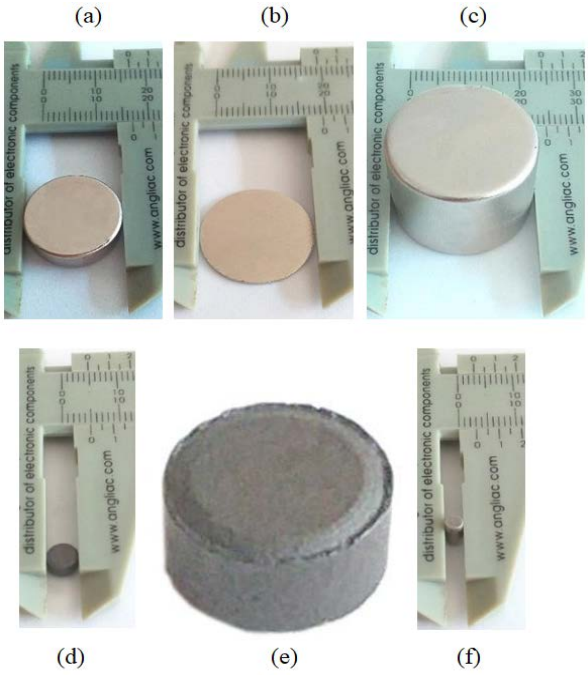

Fig. 2. Photographs of the magnets used in experiments: (a) – NdFeB, N35, $R = 8.5\,\text{mm}, L = 5\,\text{mm}$, (b) – NdFeB, N35, $R = 9.75\,\text{mm}, L = 0.5\,\text{mm}$, (c) – NdFeB, N52, $R = 12.25\,\text{mm}, L = 20\,\text{mm}$, (d) – ferrite Y10, $R = 2.5\,\text{mm}, L = 3\,\text{mm}$, (e) – magnetified view of Y10, (f) – Sm-Co, XG30, $R = 1.5\,\text{mm}, L = 5\,\text{mm}$

FEM model could take the mechanical imperfections into account. But the simulation are only as good as the input material data used to represent a given magnet grade. Simulation of magnets requires certain non-physical tricks in the FEM software [24]. Therefore, the same grade of a real magnet, the calculations performed by the analytical equations, and the FEM modelling differ to some unknown extent.

Therefore, the measurement method applied here was aimed more at detecting the forces at large distances with more accuracy, so that the magnetic dipole moments could be compared with the *Castaner* asymptote of (2). The short-distance tests are expected to be affected by friction, and thus they should be treated more as an order-of-magnitude test, rather than a precise measurement.

For these reasons, there is no single precise answer which can be used as the *absolute* reference, and therefore

Table 1. Configurations of magnet assemblies

	R (mm)	L (mm)	a (-)	B_r (T)	V (cm^3)
N35	8.5	5	0.59	1.189	1.1
N35	8.5	40	4.7	1.189	19
N35	9.75	0.5	0.051	1.189	0.039
N52	12.25	20	1.6	1.465	9.8
Y10	2.5	3	1.2	0.2175	0.059
Y10	2.5	24	9.6	0.2175	0.47
XG30 2:17	1.5	5	3.3	1.090	0.035
XG30 2:17	1.5	25	17	1.090	0.18

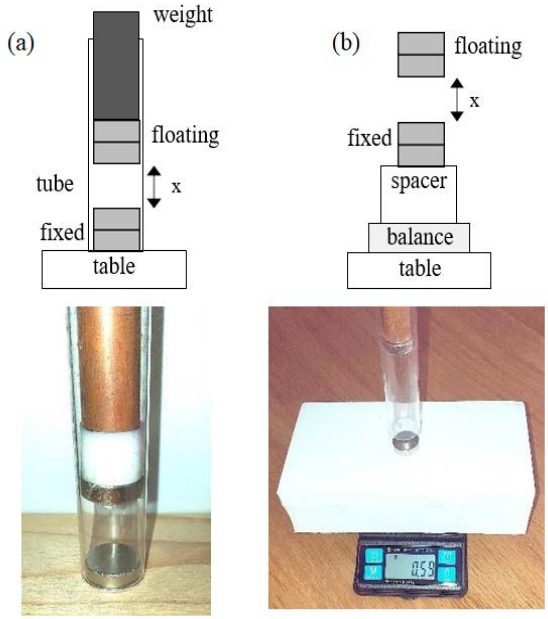

Fig. 3. Experimental setup showing "fixed" and "floating" magnets during measurements, in the: (a) – "near" region, (b) – "far" region; the photos show typical arrangement with 1+1 magnets N35 $R = 8.5\,\mathrm{mm},\ L = 5\,\mathrm{mm}$

using several values from various calculations is more meaningful when assessing the performance of analytical equations.

3.2 Description of experimental setup

Several magnet assemblies (Tab. 1) were used to investigate relatively wide range of grades, radii, aspect ratios, as well as: magnet volumes, energy and forces, with the latter three quantities spanning across three orders of magnitude. The photos of each type of magnet are shown in Fig. 2. Longer assemblies were made by stacking several magnets together, and the combined length represented the total length L of such assembly.

For small distance (large force), the bottom "fixed" magnet was rested against the wooden table (Fig. 3), and a transparent pipe was used to constrain the "floating" magnet, which was loaded with additional non-magnetic weights to reduce the floating distance and thus increase the repelling force. In this "near" region the force was derived from the total weight of the floating parts, by using the gravity $G = 9.81\,\mathrm{m/s^2}$. The distance was measured with a non-magnetic calliper (the one pictured in Fig. 2), but the practical resolution was limited to around 0.5 mm because of measuring through the pipe wall. Each pipe had a slightly larger diameter than the given magnet type so that the friction was minimized, an approach similar to that used in [9].

For large distance (small forces), the bottom magnet was put on a separating block (50 mm thick), on an electronic balance with 0.01 g resolution. Some components inside the balance (batteries) contained ferromagnetic metals and could affect the readings, so the separating block reduced the errors to less than the measurable 0.01 g resolution.

Because the floating magnet was suspended much farther above the fixed magnet, any additional force acting directly on the balance was also negligible. The same plastic tube was used to provide axial alignment, but it was suspended just above the fixed magnet so that there was no impact on the weight measured by the balance (*eg* by accidental touching). Sticky tape (0.04 mm thick) was used to suspend the floating magnets.

In the "near" region the measurement were expected to be "noisy" due to the unknown effect of friction. However, in the "far" region the measurement can be deemed to be more precise, because the force was measured directly by the balance. The free-floating distance for a given magnet dictated the transition between the "near" region (just more weights added), and the "far" region (suspend the magnet and move it higher).

4 Comparison of results

For brevity, only a comparison of the extreme cases of aspect ratio for each type of magnet is included below, because for the intermediate values (which were also measured) the behaviour fell between the extremes reported herein.

4.1 NdFeB, N35, $R = 8.5\,mm$, $L = 5\,mm$, $a = 0.59$

As expected, the simplest curve *Castaner* gives results which are only reasonable for large distances, but diverges to infinity near zero (Fig. 4), and errors are begin to grow quickly for $x < 10L$. Similar behaviour is for *Furlani*, albeit with a slower divergence. For this relatively small aspect ratio *Cheedket* only works well for large distances, but fails to predict a correct value of force at $x = 0$ and it becomes even worse for lower aspect ratios, as shown in the following subsections.

The *new* equation produces reasonable values over the whole range, and being based on Furlani, it converges to the $1/x^4$ slope, together with *Castaner*, *Furlani*, *Cheedket*, FEM, and *Supermagnete*.

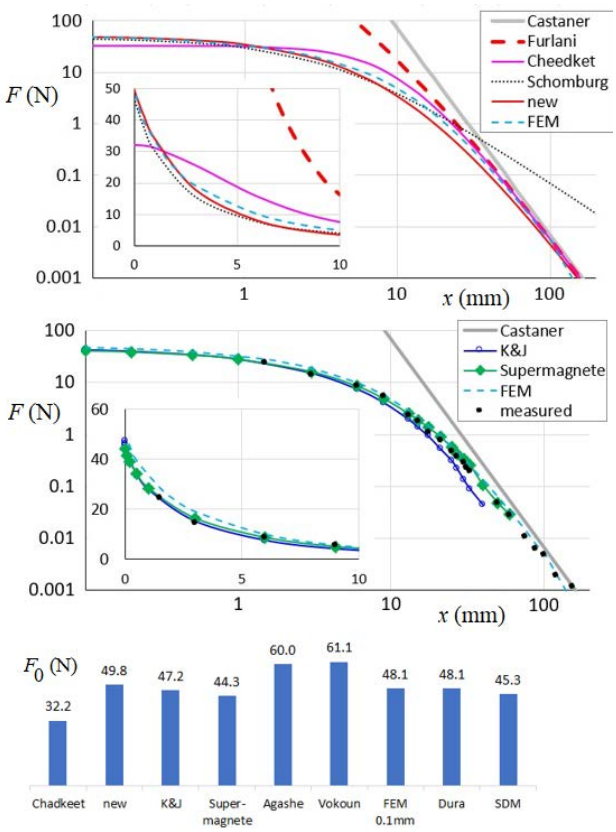

Fig. 4. Comparison for NdFeB, N35, $R = 8.5\,\text{mm}$, $L = 5\,\text{mm}$, $a = 0.59$, for curves (top and middle) and contact force (bottom); the curves are split over two graphs for better clarity, and the insets show the same data but with linear rather than logarithmic scales

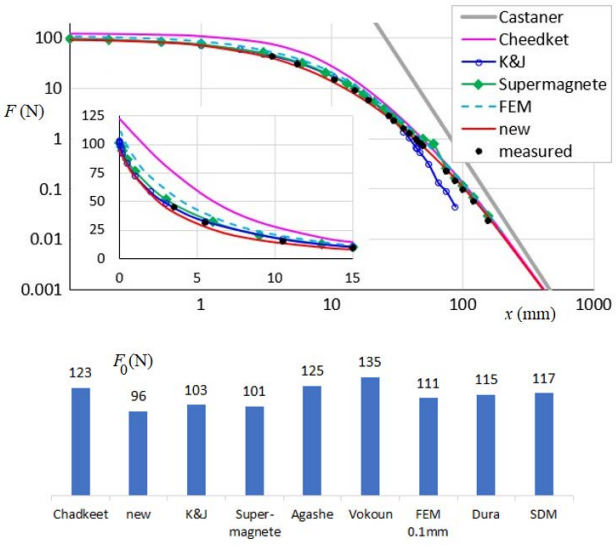

Fig. 5. Comparison for NdFeB, N35, $R = 8.5\,\text{mm}$, $L = 40\,\text{mm}$, $a = 4.7$

Schomburg provides reasonable approximation for large forces, but only after furnishing it with the F_0 and d_e values from $K\&J$. It fails completely at large distance as could be expected. Both $K\&J$ and *Supermagnete* agree very well with each other for small distances, but $K\&J$ underestimates force at large separation, and thus fails to converge to *Castaner*.

Agashe and *Vokoun* overestimate the contact force, as compared to all others. *Cheedket* reports the lowest value, due to low aspect ratio. The contact force for *new* agrees reasonably with $K\&J$, *Supermagnete*, and FEM.

The measured force follow the expected curve shapes, tending to some limited value (but not possible to measure at exactly $x = 0$ with the employed setup), and for large distances also approaching the asymptote, confirming that the point-like dipole approximation with (1) is correct at large distances.

For sake of clarity and compactness, curves *Furlani* and *Schomburg* are omitted in the next graphs, but *Castaner* is used as the asymptote for large distances.

4.2 NdFeB, N35, $R = 8.5\,mm, L = 40\,mm, a = 4.7$

For this larger aspect ratio, *Cheedket* overestimates the contact force (as compared to $K\&J$, Supermagnete and FEM), and $K\&J$ again underestimates failing to approach the asymptote (Fig. 5). The *Cheedket*, *new*, and *measured* curves approach the *Castaner* limit. Again, contact forces of *Agashe* and *Vokoun* are higher than others.

4.3 NdFeB, N35, $R = 9.75\,mm, L = 0.5\,mm, a = 0.051$

For such a small aspect ratio (Fig. 6), *Cheedket* severely underestimates the contact force, even reducing as x approaches zero, which clearly does not reflect the shape of a force curve between real magnets. Compared to $K\&J$ data at small distances, the *new* prediction is least incorrect.

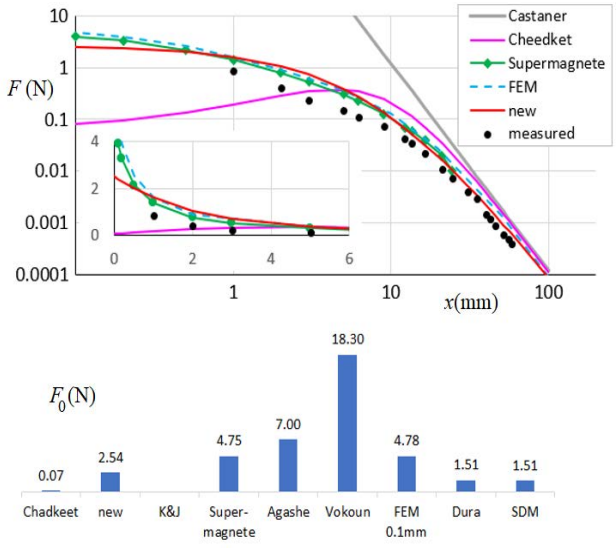

Fig. 6. Comparison for NdFeB, N35, $R = 9.75\,\text{mm}$, $L = 0.5\,\text{mm}$, $a = 0.051$

It should be noted that for large distances, the measured values begin to follow a slope which is parallel to the *Castaner* limit, but visibly lower. This indicates that the real magnetic dipole moment is lower that the assumed ideal, which can be expected for such flat magnets. Their thickness was only 0.50 mm, but if they were coated with 0.03 mm on each side this constitutes over 10% change in the magnet volume (first contribution to lower forces) and unknown amount of "short- circuiting" of magnetic flux around the magnet (another contribution to lower forces).

For such small aspect ratio, *Agashe* reports much higher contact force, but the approximated *Vokoun* is severely affected.

4.4 *NdFeB, N52,* $R = 12.25\,mm, L = 20\,mm, a = 1.6$

These were the highest-energy magnets used in this study. Throughout the range, but especially at large distances (Fig. 7) the *measured* values are significantly lower than the expected ideal limit.

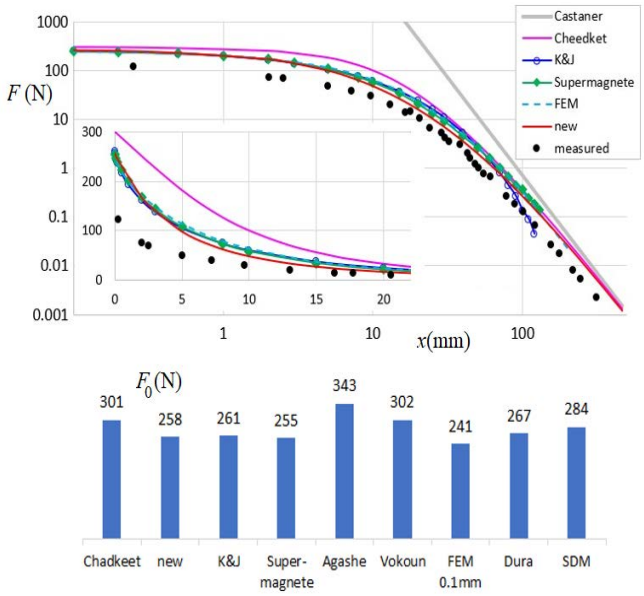

Fig. 7. Comparison for NdFeB, N52, $R = 12.25\,\text{mm}, L = 20\,\text{mm}, a = 1.6$

These magnets have rounded corners, see also Fig. 2(c), which must contribute to the real forces being lower. However, the author suspects that the magnets had lower grade than the advertised N52 (possibly even below N35), and this is a possibility, since they procured from an internet shop.

Again, *Cheedket* clearly overestimates the curve for smaller distances, but new conforms better to $K\&J$, Supermagnete, and FEM.

4.5 *Ferrite, Y10,* $R = 2.5\,mm, L = 3\,mm, a = 1.2$

This configuration resulted with the lowest forces. Because of the ferrite material it was not possible to get the values for $K\&J$, *Supermagnete*, and *Dura*, Fig. 8. Therefore, the only reference was provided by FEM, with which the *measured* and *new* curves agreed quite well, especially away from direct contact.

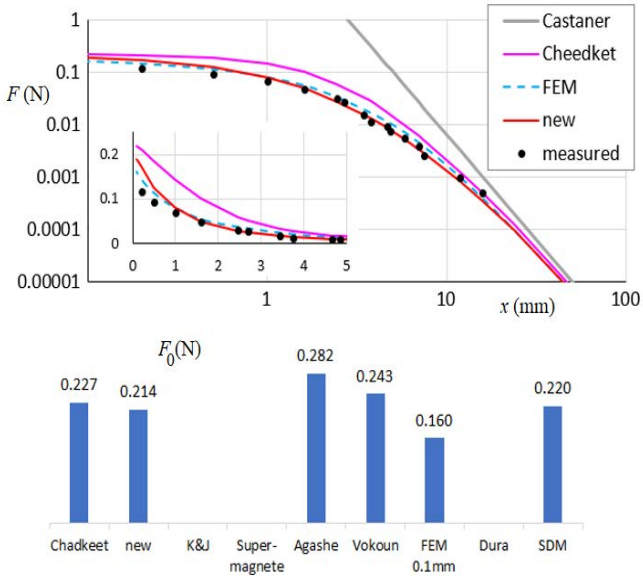

Fig. 8. Comparison for ferrite, Y10, $R = 2.5\,\text{mm}, L = 3\,\text{mm}, a = 1.2$

4.6 *Ferrite, Y10,* $R = 2.5\,mm, L = 24\,mm, a = 9.6$

With a longer ferrite magnet assembly, *Vokoun* value changes from being lower than *Agashe* (Fig. 8) to being highest of all (Fig. 9). Other values follow similar trends as in Fig. 8.

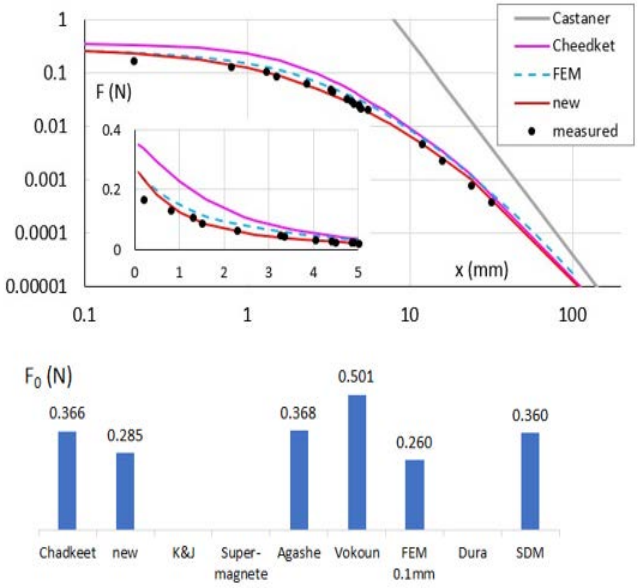

Fig. 9. Comparison for ferrite, Y10, $R = 2.5\,\text{mm}, L = 24\,\text{mm}, a = 9.6$

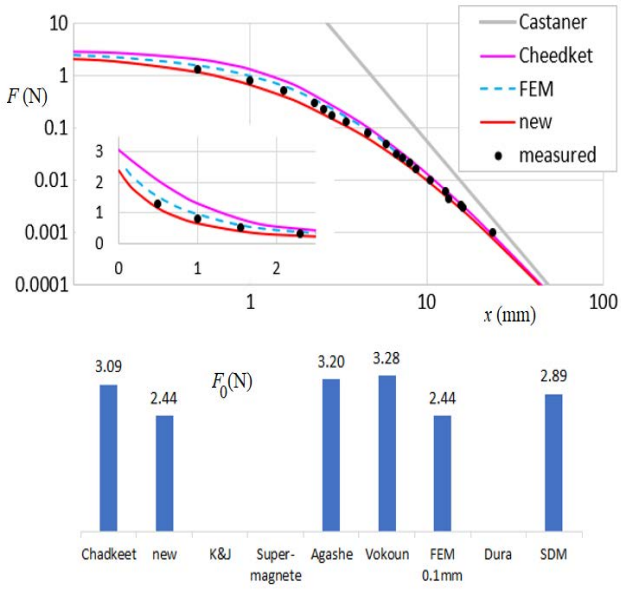

Fig. 10. Comparison for SmCo, XG30, $R = 1.5$mm, $L = 5$mm, $a = 3.3$

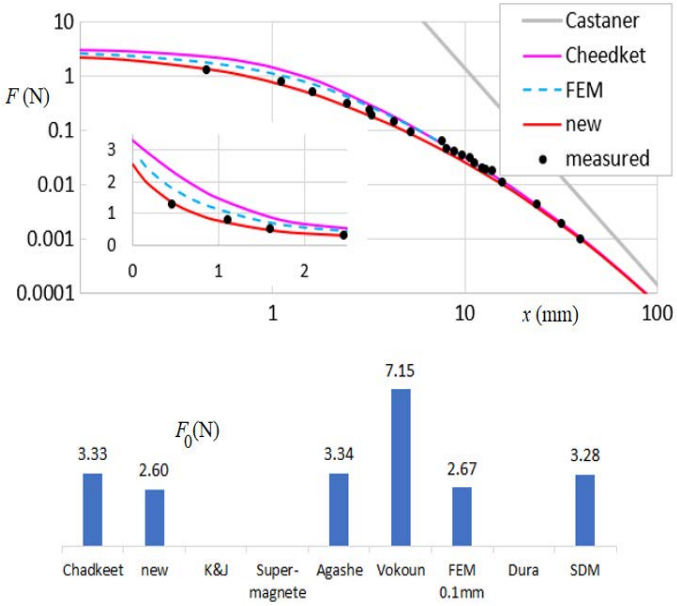

Fig. 11. Comparison for SmCo, XG30, $R = 1.5$ mm, $L = 25$ mm, $a = 17$

4.7 SmCo, XG30 2:17, $R = 1.5\,mm, L = 5\,mm, a = 3.3$

The SmCo magnets were chosen to have a large aspect ratio. They had relatively high energy (grade XG30) but their small volume resulted in small forces (Fig. 10). Again, not being NdFeB magnets it was not possible to obtain the forces for *K&J*, *Supermagnete*, and *Dura*.

4.8 SmCo, XG30 2:17, $R = 1.5\,mm$, $L = 25\,mm$, $a = 17$

Because of the slender shape, using the same magnets in a much longer configuration did not significantly increase the forces acting in the short range (Fig. 11, as compared to Fig. 10). However, the length of the dipoles was increased and thus it was more difficult to approach the *Castaner* limit, because much larger distances would be required (and which extended beyond the capability of the measurement setup). *Vokoun* significantly overestimates the contact force.

5 Summary and conclusions

There are significant discrepancies between the force values provided by the manufacturers and suppliers of magnets, those computed by numerical methods such as FEM, and those calculated by closed-form analytical equations. Therefore, it is not possible to provide an absolute reference which can be used under all conditions.

However, the performance of analytical curves and analytical equations for contact force values can be judged on their qualitative behaviour over a wide range of input values. The approximations via magnetic dipoles *Castaner*, (2) or surface charges *Furlani* (3), diverge to infinity for zero separation between magnets. Equation (4) (*Cheedket*) behaves less incorrectly, providing some value of contact force, but it overestimates the values for large aspect ratio ("long" magnets) and severely underestimates the contact force for small aspect ratio (coin-like "flat" magnets).

Equation (5) (*Schomburg*) gives reasonable curve fitting, but only for small distances, and is inherently unable to provide *a priori* the contact force value, unless real measurements are made, or other calculations are made first.

The *new* proposed analytical closed-form equation (6) is relatively simple because it is directly based on (3) (*Furlani*). It is not derived in any strict way, but it provides the most reasonable approximation as compared to the reference data of measurements and FEM simulations, over the entire studied range of values: separation distance, magnet volume and aspect ratio, as well as forces.

Acknowledgements

The author thanks Mrs. J. Kaczmarzyk for support during the experimental measurements, as well as Mrs. Z. Szozda and Prof. M. Soinski for inspiration for this study.

References

[1] J. S. Agashe and D. P. Arnold, "A study of scaling and geometry effects on the forces between cuboidal and cylindrical magnets using analytical force solutions", *Journal of Physics D: Applied Physics*, vol. 41, no. 10, pp. 105001 doi: stacks.iop.org/JPhysD/41/105001, 2008.

[2] R. Ravaud, "Cylindrical Magnets and Coils: Fields, Forces, and Inductances", *IEEE Transactions on Magnetics*, vol. 46, no. 9, pp. 3585-3590 doi: 10.1109/TMAG.2010.2049026, 2010.

[3] D. Vokoun *et al*, "Magnetic forces between arrays of cylindrical permanent magnets", *Journal of Magnetism and Magnetic Materials*, pp. 323, pp. 55-60 doi:10.1016/j.jmmm.2010.08.029 2011, 2011.

[4] J. M. Camacho and V. Sosa, "Alternative method to calculate the magnetic field of permanent magnets with azimuthal symmetry", *Revista Mexicana de Fisica*, vol. 59, pp. 8-17, 2013.

[5] Y. Zhang *et al*, "Comparative study on equivalent models calculating magnetic force between permanent magnets", *Journal of Intelligent Manufacturing and Special Equipment*, vol. 1, no. 1, pp. 43-65 doi: 10.1108/JIMSE-09-2020-0009, 2020.

[6] S. Liu and F. L. Duan, "Study of Interactive Force between Two Permanent Magnets", *TechRxiv*, doi: 10.36227/techrxiv.19786474.v1, 2022.

[7] W. K. Schomburg *et al*, "Equations for the approximate calculation of forces between cuboid magnets", *Journal of Magnetism and Magnetic Materials*, . 506, 166694, doi: 10.1016/j.jmmm.2020.166694, 2020.

[8] D.C. Jiles, *Introduction to Magnetism and Magnetic Materials*, 2-nd edition, Chapman & Hall, crc. 2, ISBN 9780412798603, 1998.

[9] R. Castaner, "The magnetic dipole interaction as measured by spring dynamometers", *American Journal of Physics*, vol. 74, no. 6, pp. 510-513, doi: 10.1119/1.2180286, 2006.

[10] K. W. Yung *et al*, "An analytical solution for the force between two magnetic dipoles", *Magnetic and Electrical Separation*, no. 9, pp. 39-52,.

[11] E. P. Furlani, *Permanent magnet and electromechanical devices*, ISBN 0122699513, 2001.

[12] J. G. Ku *et al*, "Interaction between two magnetic dipoles in a uniform magnetic field", *AIP Advances*, no. 6, pp. 025004 doi: 10.1063/1.4941750, 2016.

[13] S. Cheedket and C. Sirisathitkul, "Comparison of closed-form solutions to experimental magnetic force between two cylindrical magnets", *EUREKA: Physics and Engineering*, no. 4, pp. 125-130, doi: 10.21303/2461-4262.2021.001955, 2021.

[14] D. Vokoun *et al*, "Magnetostatic interactions and forces between cylindrical permanent magnets", *Journal of Magnetism and Magnetic Materials*, vol. 321, pp. 3758-3763, doi:10.1016/j.jmmm.2009.07.030, 2009.

[15] J. S. Agashe and D. P. Arnold, "Corrigendum: A study of scaling and geometry effects on the forces between cuboidal and cylindrical magnets using analytical force solutions", *Journal of Physics D: Applied Physics*, pp. 1, 2009.

[16] S. Zurek, *Closed-form approximation of complete elliptic integrals, Encyclopedia Magnetica*, https://www.e-magnetica.pl/approximation_of_complete_elliptic_integrals.

[17] ChenYang Technologies, *Calculation of Pull Force between two DiscMag nets*, http://www.cy- magnetics.com/PullForce-DiscMagnets.htm.

[18] *K&J* Magnetics, *The K&J Repelling Magnet Calculator*, https: //www.kjmagnetics.com/calculator.repel.asp.

[19] S. Maxwell, "*K&J* Magnetics", *private communication*,.

[20] J. Cheah, *Magnetic Forces Between Two Permanent Magnets*, https://www.ansystips.com/2017/04/magnetic-forces-between-two-permanent.html, 2017.

[21] Supermagnete, *Adhesive Force Calculation*, https://www.supermagnete.de/eng/adhesive-force-calculation.

[22] Dura Magnetics, *Neodymium Magnetic Pull Force Calculator*, https://www.duramag.com/neodymium-magnets- ndfeb/neodymium-magnetic-pull-force-calculator/.

[23] SDM Magnetics, *Pull Force Calculators*, https://www.magnet-sdm.com/pull-force-calculators.

[24] D. Meeker, *Finite Element Magnetics Method, FEMM*.

[25] Arnold Magnetic Technologies, *Neodymium Iron Boron Magnet Catalog*, https://www.arnoldmagnetics.com/wp-content/uploads/2019/06/Arnold- Neo-Catalog.pdf, 2019.

Received 17 October 2022

Stan Zurek graduated with MSc at Czestochowa University, Poland in 2000, PhD at Cardiff University, UK in 2005, and DSc at Łodz University, Poland in 2020, specializing in measurements of rotational magnetization in soft magnetic materials. He is an author and co-author of over 100 scientific and technical papers, author of a book Characterisation of soft magnetic materials under rotational magnetisation published in 2017 by Taylor & Francis/CRC Press, and a co-inventor of 13 patents. He became a Senior Member of IEEE in 2010, Charted Engineer in 2020, and a Fellow of IET in 2022. He currently holds the position of Head of Research and Innovation in Megger Instruments, Dover, UK. He is also an Editor-in-Chief of Encyclopedia Magnetica.